Available online at www.sciencedirect.com
SCIENCE DIRECT®
Earth and Planetary Science Letters 243 (2006) 504–519
EPSL
www.elsevier.com/locate/epsl

Isotope calibrated Greenland temperature record over Marine Isotope Stage 3 and its relation to CH_4

Christof Huber [a,1], Markus Leuenberger [a,*], Renato Spahni [a,2], Jacqueline Flückiger [a,b,3], Jakob Schwander [a,2], Thomas F. Stocker [a,4], Sigfus Johnsen [c,5], Amaelle Landais [d,e,6], Jean Jouzel [d,7]

[a] *Climate and Environmental Physics, Physics Institute, University of Bern, Sidlerstrasse 5, CH-3012 Bern, Switzerland*
[b] *Institute of Arctic and Alpine Research, University of Colorado at Boulder, 450 UCB, Boulder, Colorado 80309-0450, USA*
[c] *Department of Geophysics, Juliane Maries Vej 30, University of Copenhagen, DK-2100, Copenhagen, Denmark*
[d] *IPSL/Laboratoire des Sciences du Climat et de l'Environnement, UMR CEA-CNRS, CEA Saclay, 91191 Gif-sur-Yvette, France*
[e] *Institute of Earth Sciences, Hebrew University, 93183 Jerusalem, Israel*

Received 28 June 2005; received in revised form 30 November 2005; accepted 5 January 2006
Available online 21 February 2006
Editor: E. Boyle

Abstract

Large temperature variations on millennial time scales in Greenland characterised the last ice age. Abrupt warmings, known as Dansgaard–Oeschger (DO) events, can be traced in the $\delta^{18}O_{ice}$ record of Greenland ice cores. However, it has been shown that $\delta^{18}O_{ice}$ is not a direct temperature proxy. Measurements of the isotopic composition of gases trapped in the ice can be used to calibrate the paleothermometer. Here we present a continuous temperature record based on high resolution $\delta^{15}N$ measurements and firn model studies. It covers a sequence of 9 DO events (9–17) during the time period from 38 to 64 kyr BP for which temperature changes of 8 to 15 °C were estimated. The difference between the modern and the glacial $\delta^{18}O_{ice}$–T relationship can be explained by a combination of source temperature changes and changes in the annual distribution of precipitation. A detailed comparison of the temperature evolution with reconstructions of the atmospheric methane (CH_4) concentration shows that CH_4 rises lag temperature increases at the onset of DO events by 25 to 70 yr within data resolution. The strong correlation between Greenland temperature and CH_4 on millennial and submillennial time scales suggests that variations on these time scales were probably of hemispheric extent.

Keywords: Marine Isotope Stage; Dansgaard-Oeschger events; Greenland; Methane; Ice age

* Corresponding author. Tel.: +41 31 631 44 70; fax: +41 31 631 87 42.
E-mail addresses: Christof.Huber@flowtec.endress.com (C. Huber), leuenberger@climate.unibe.ch (M. Leuenberger), spahni@climate.unibe.ch (R. Spahni), flueckiger@colorado.edu (J. Flückiger), schwander@climate.unibe.ch (J. Schwander), stocker@climate.unibe.ch (T.F. Stocker), sigfus@gfy.ku.dk (S. Johnsen), landais@vms.huji.ac.il (A. Landais), jouzel@lsce.saclay.cea.fr (J. Jouzel).
[1] Tel.: +41 31 631 85 64; fax: +41 31 631 87 42.
[2] Tel.: +41 31 631 44 76; fax: +41 31 631 87 42.
[3] Tel.: +1 303 735 5850; fax: +1 303 492 6388.
[4] Tel.: +41 31 631 44 62; fax: +41 31 631 87 42.
[5] Tel.: +45 353 20558.
[6] Tel.: +972 2 65 84246; fax: +972 2 56 62581.
[7] Tel.: +33 1 69 08 77 13; fax: +33 1 69 08 77 16.

0012-821X/$ - see front matter © 2006 Elsevier B.V. All rights reserved.
doi:10.1016/j.epsl.2006.01.002

1. Introduction

The climate over the last glacial period was characterised by numerous abrupt climate changes known as Dansgaard–Oeschger (DO) events [1]. They can be traced in paleorecords from the Arctic ice sheets, as well as from tropical and subtropical regions [2–5]. DO events are most prominently represented in $\delta^{18}O_{ice}$, the oxygen isotope ratio in Greenland ice cores. They have been related to shifts of the ocean thermohaline circulation (THC) [6–8]. DO events in Greenland typically start with a rapid warming of about 8 up to 16 °C within a few decades [9–12] followed by a more gradual cooling phase over several centuries and a rapid drop back towards cold stadial conditions. The long lasting DO events were preceded by massive ice surges from the northern ice sheets, documented by debris deposits at the ocean floor known as Heinrich (H) events [13].

Water isotopes in ice cores ($\delta^{18}O_{ice}$ or δD) are useful temperature proxies because changes in isotopic composition of precipitation in polar regions are mainly related to variations of temperatures at the site of precipitation. The present day spatial relationship between $\delta^{18}O_{ice}$ and temperature, $\alpha_{spatial}$, is estimated at 0.67‰/K for Greenland [14]. α depends on variations of the seasonal precipitation distribution [17] and/or changes occurring at the source region [18,19] of precipitation. Therefore, the present day $\alpha_{spatial}$ cannot be used to quantitatively interpret past climate shifts [15,16].

Measurements of the isotopic composition of nitrogen $\delta^{15}N$ and/or argon $\delta^{40}Ar$ on air trapped in ice cores can be used to calibrate the $\delta^{18}O_{ice}$ to temperature relation, during an event of rapid temperature change [9–12,20–22]. Because atmospheric $\delta^{15}N$ is constant [23], changes of this air parameter trapped in ice indicate fractionations due to gravitation and thermal diffusion [24]. Rapid warming or cooling at the surface produces a temperature gradient in the firn that forces the heavier isotopes to migrate towards the cold end. This results in an alteration of the isotope signal trapped in the ice core. The surface temperature change can be reconstructed by comparing the measured isotope fractionation with firn gas diffusion model calculations. This approach has been used to deduce rapid temperature changes for several DO events [9–12,20,24,25] during the last glacial epoch.

Here we present a reconstruction of the temperature evolution over 9 consecutive DO events (events 9 to 17) during Marine Isotope Stage (MIS) 3, based on high resolution $\delta^{15}N$ measurements on the ice core from the North Greenland Ice Core Project (NorthGRIP) [26], using a new on-line technique [27,28]. This record is compared with existing high resolution CH_4 measurements from the NorthGRIP [29] (DO 9–12), and the GISP2 [31,30] (DO 9–17) ice cores. Additionally, we present new highly resolved CH_4 measurements from the NorthGRIP ice core for the time period of DO 15–17. This allows us to compare in detail methane and reconstructed temperature evolutions over a longer time period including rapid temperature variations (DO 9–17).

2. Method

Firn, the porous upper 50–100 m of an ice sheet, can be divided into three zones from top to bottom: (i) The convective zone, where the air is well mixed with the atmosphere; (ii) The diffusive column, where the isotopic and elemental composition of the air is altered by diffusion, such as gravitational settling [32,33] and thermal diffusion [9,20,24]; (iii) The non-diffusive zone, where no vertical mixing of the air occurs.

Isotopic enrichment due to gravitational fractionation, e.g. of $\delta^{15}N$, at the bottom of the diffusive column can be calculated using the barometric equation [32,33]:

$$\delta(z) = \left(e^{(\Delta mgz/RT)} - 1\right) \cdot 1000‰ \cong \Delta m \cdot g \cdot z/(R \cdot T) \cdot 1000‰ \quad (1)$$

where Δm is the mass difference between the isotope species, T is the mean firn temperature, z is the firn depth, g the Earth gravitational acceleration, and R the ideal gas constant. Hence, for stable climatic conditions the diffusive column height (DCH) is rather constant and can be obtained from nitrogen or argon isotope ratios measured in the ice core. The second process that alters the isotopic composition of the air in the firn diffusive column is thermal diffusion:

$$\delta = \left[\left(\frac{T_t}{T_b}\right)^{\alpha_T} - 1\right] \cdot 1000‰ \cong \Omega \cdot \Delta T \quad (2)$$

where ΔT is the temperature difference between the top (T_t) and the bottom (T_b) of the diffusive column, α_T is the thermal diffusion constant, and Ω the thermal diffusion sensitivity (‰/K). The latter two parameters depend on the mean firn temperature [20]. Gratchev and Severinghaus [34] measured the thermal diffusion sensitivity of nitrogen isotopes. An abrupt surface temperature increase, e.g., at a DO event, causes a temperature gradient in the firn column. In this case ^{15}N is enriched over ^{14}N at close off depth (Eq. (2)) because gas diffusion is about 10 times faster than temperature

diffusion in the firn [35,36]. Temperature diffusion re-establishes a uniform temperature profile after a few centuries whereby the fractionation disappears.

These two effects can be quantified by nitrogen and argon isotope measurements on the same air sample. As for nitrogen, argon has constant atmospheric isotopic composition.

The gravitational signal of $\delta^{15}N$ and $\delta^{40}Ar/4$ is identical, but the thermal diffusivities are different. Hence, the temperature gradient in the firn is proportional to $\delta^{15}N_{excess}=\delta^{15}N-\delta^{40}Ar/4$ [10,11]. By measuring both parameters, $\delta^{15}N$ and $\delta^{40}Ar$, on air extracted from Greenland ice cores, the magnitude of abrupt temperature changes can be estimated [10–12,21]. One prerequisite for this method is the availability of accurate values for the thermal diffusion constants [34,37].

The precision of our argon data is too low for the $\delta^{15}N_{excess}$ calculation [28] therefore, we are forced to follow an alternative approach. A combined firn densification/temperature/gas diffusion model [36,22] is used to calculate the evolution of $\delta^{15}N$ in a forward model sense, using an assumed temperature and snow accumulation rate history. The model results are then compared to the measurements [9,20]. Three model approaches (approach 1, 2 and 3) are explained in detail in the Appendix. Both methods, the $\delta^{15}N_{excess}$ and our model approach, are subjected to uncertainty in estimating temperature variations when the existence of a significant convective zone (≥ 10 m) cannot be excluded. This is because the convective zone lowers the thermal gradient that causes the $\delta^{15}N$ or the $\delta^{15}N_{excess}$ signal. When this effect is not accounted for, both methods tend to underestimate the temperature changes (see Appendix A.1. for more details).

The validity of our model approach has been checked for different DO events. For DO 19 the abrupt temperature change of 16 °C determined with the model-approach on the GRIP ice core [9] has been confirmed with the $\delta^{15}N_{excess}$-approach on NorthGRIP ice [12]. Additionally, on DO 12 the converse way of confirmation was performed using the $\delta^{15}N_{excess}$ method on GRIP ice [11] and our model approach on NorthGRIP ice (this study). Even the observed long term offset in $\delta^{18}O_{ice}$ during the glacial period in contrast to the Holocene [26] cannot weaken this confirmation using different cores from Greenland for two reasons: (i) the signals for rapid changes agree well during the glacial and (ii) the difference of $\delta^{18}O_{ice}$ records from NorthGRIP and GRIP does not exhibit variations associated with DO events. Apparently, the latitudinal temperature sensitivity does not change much on centennial to millennial time scales in contrast to longer time scales (10 kyr) between those two sites.

Another test of the validity of both methods was performed by a direct comparison of the two methods for DO events 18, 19 and 20 using the measurements of Landais et al. [12]. They showed that their surface temperature scenario and firnification model were able to reproduce both $\delta^{15}N_{excess}$ and $\delta^{15}N$ with a small convective zone of 2 to 5 m for both the GRIP and NorthGRIP location. Therefore, we assumed no convective zone. This is supported by our results from the convective zone approach (see below and Appendix A.1., Fig. 8) where no correlation between DO events and reconstructed convective zone depth is obtained. First, we compared results of two different firn densification/temperature/gas diffusion models [36,22] and found no significant differences for the same input values. Second, we ran our model for different input values in order to match $\delta^{15}N$ values of Landais et al., [12]. Different scenarios are given in Fig. 1. For the scenario with a reduced accumulation rate as used for DO events 9–17 (see below), the model $\delta^{15}N$ does not match the data (cyan line). A good agreement can be reached for higher accumulation

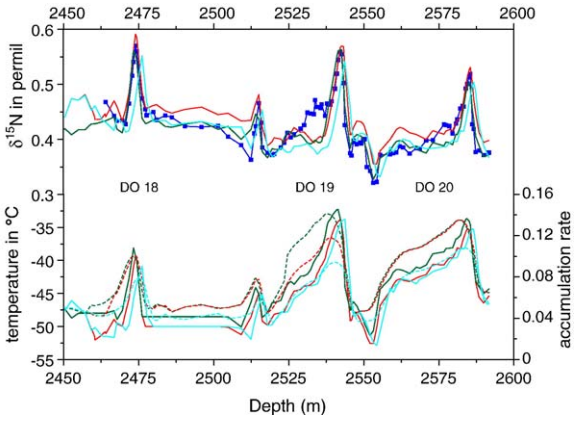

Fig. 1. (Top panel) $\delta^{15}N$ data of NorthGRIP obtained by Landais et al. [12] (blue squares) as well as modelled $\delta^{15}N$ for different scenarios plotted against depth. (Bottom panel) Corresponding temperature evolution (solid lines) and accumulation rates (dashed lines). Temperature evolution obtained by Landais et al. [12] based on $\delta^{15}N_{excess}$ method (red line) using the ss09sea accumulation rate, same temperature evolution but 20% reduced accumulation rate (cyan line, this study) and tuned temperature and accumulation rate (green line, this study). The mismatch between the reduced accumulation rate scenario (cyan line) with the data documents that the reduced accumulation rate scenario is not adequate. The tuned scenario is very similar to the $\delta^{15}N_{excess}$ scenario however shifted by −1.5 °C. Increased accumulation rates could be responsible for the significant mismatch during the end of DO 19 as indicated by the green dashed line due to an deepening of the close-off depth.

rates, except for the end of DO 19 (green line). However, this is also the case for the $\delta^{15}N_{excess}$ approach. The temperature evolution (green line) is consistent with the results obtained by the $\delta^{15}N_{excess}$ method documenting the validity of both approaches. The independent temperature estimates are well within the assigned temperature uncertainty of ±3 °C derived from $\delta^{15}N$ alone.

The model input is the surface temperature, T_s, and the accumulation rate. Accumulation strongly depends on temperature. Hence it can be related to $\delta^{18}O_{ice}$ [16] by an empirical relation determined for present day conditions. However, the relations of the temperature as well as of the accumulation to $\delta^{18}O_{ice}$ are not well known for glacial conditions. This is documented by significantly different accumulation estimates for GRIP and GISP2 [16,38]. In our model we tuned both parameters (surface temperature and the accumulation rate) in order to minimize the squared deviations between the model and the measured $\delta^{15}N$. A detailed description of the fitting procedure is given in Appendix A, where different approaches, which have been used to deduce past temperature evolution from our NorthGRIP $\delta^{15}N$ data, are discussed and compared with each other. This leads to two conclusions. The relation between temperature and $\delta^{18}O_{ice}$ is not linear and should be revised. Our findings support a more complex relationship that is influenced most probably by varying seasonal precipitation distribution and changes of the precipitation source region. The best fit is achieved by reducing the accumulation rates by 20% compared to the assumptions made in the ice flow dating model for the NorthGRIP ss09 sea age scale [39,26]. In order to preserve the depth-to-age relation of the NorthGRIP ice core that is independently determined [39], the ice thinning function has to be changed accordingly.

The tuning procedure (iteration) yields the temperature evolution over the observed time period. A good agreement between model and measurements is obtained for the magnitude of the $\delta^{15}N$ fractionation as well as for the timing of the events (Fig. 2). This suggests that the relation between accumulation rate and temperature used in the model is a reasonable choice. Hence, we obtain a good estimate for the ice-age to gas-age difference (Δage) which, however, is dependent on the age scale used. Even more important is a comparison of measured and modelled Δdepths that are not dependent on the used age scale. This leads to a reconstructed temperature record from $\delta^{15}N$ values and allows us to compare it to CH_4 within the time resolution of ±25 yr of the records. Note that different absolute temperature levels, as much as 5 °C (see Appendix A.2.), are expected due to model dependencies on the assumed accumulation rate and the convective zone depth but with minor influence on the rapid temperature changes. An increase of 3.5 °C corresponds to a reduction of the diffusive column height of 10 m and therefore a reduced $\delta^{15}N$ of 0.05‰, it does however lead to a mismatch of model and measured Δdepths. This can be compensated by a reduced accumulation rate history associated with a corresponding change in the thinning function as mentioned above (see Appendix A.3. for details).

Independent of the mean temperature level, the amplitude of rapid temperature changes can be determined with a precision better than ±3 °C, corresponding to the 95% confidence interval (2σ). This error is determined using Monte Carlo simulations (see Appendix A) and originates primarily from the analytical uncertainty of the $\delta^{15}N$ measurements of ±0.02‰ ($\pm 2 \times 0.02‰ / \Omega =$ ±2.9 °C, where Ω is the thermal diffusion sensitivity, with a value of 0.014‰/°C at −50 °C [34]).

It has to be mentioned that if large convective zones (≥10 m) exist during cold stages — for instance due to increased wind-pumping—then rapid transitions from cold to warm stages could lead to an abrupt decrease of those convective zones mimicking rapid temperature increases due to a lowering of wind-pumping. This effect is not accounted for in our present model and would also not be compensated by the slower adjustment towards shallower close-off depths. Such a scenario seems to be rather unlikely since calculated convective zone evolution via the mismatch of model and measured $\delta^{15}N$ does not show a correlation with the rapid DO events (see Appendix A.1., Fig. 8). Nevertheless, it cannot be ruled out.

Therefore, we decreased the lower uncertainty limit due to this effect during rapid changes by additional 3 °C, corresponding to a change of nearly 10 m in the convective zone height. This effect may lead to lower temperature shifts as assigned in Fig. 2 based on our assumption of a non-existing convective zone. Hence, the temperature sensitivity for rapid changes would decrease between GRIP and NorthGRIP in contrast to general findings with increasing latitude. It would, however, explain the disagreement between model and measured $\delta^{15}N$ values, but the discrepancy in Δdepths would still remain and therefore favours our approach 3 as discussed in the Appendix of a reduced accumulation. Improvements

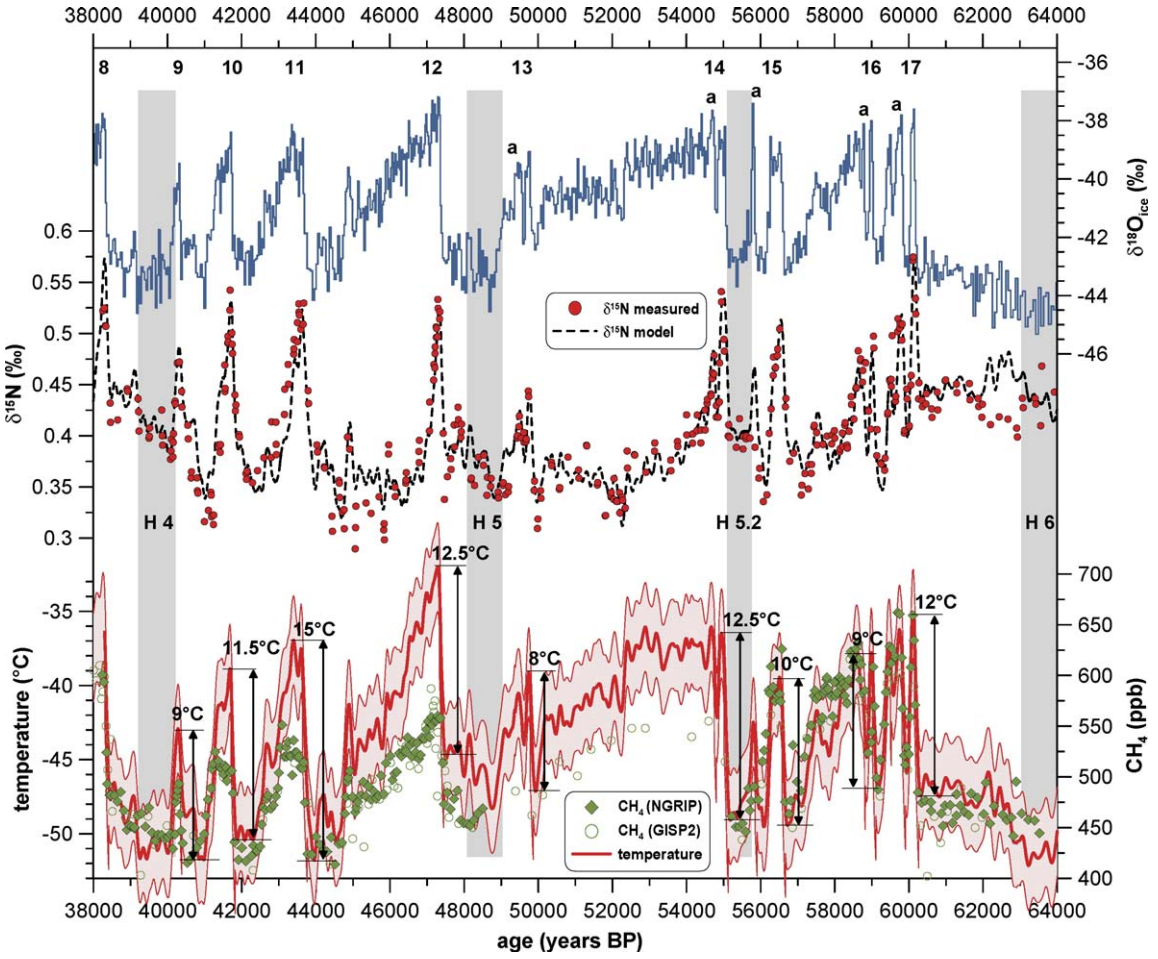

Fig. 2. (Top panel) NorthGRIP $\delta^{18}O_{ice}$ [26], (middle panel) NorthGRIP $\delta^{15}N$, (bottom panel) surface temperature (solid line), and CH_4 concentration from NorthGRIP [29] (filled diamonds) and GISP2 [50] (open circles), for the time period of DO 8–17 (38 to 64 kyr BP). All curves are plotted on the GRIP2001/ss09sea [39,26] age scale. $\delta^{15}N$ measurements (dots) are compared to a model curve (dashed line). The temperature curve is deduced by fitting a firn densification and heat diffusion model [36] to the $\delta^{15}N$ data. Temperature is plotted as smoothed line (50 yr). Upper and lower uncertainty limits (2 σ) are given. They are not symmetric during DO events due to potential influences of rapid changes of the convective zone which could mimic temperature variations (for details see text) and hence would result in an enhanced temperature shift. Temperature changes associated with DO events are marked for each event except for DO 8 which could not be interpreted, due to the lack of $\delta^{15}N$ measurements. Heinrich (H) events are marked as shaded bands [13].

of these estimates could be obtained by measuring argon isotopes.

3. Results and discussion

3.1. Greenland temperature evolution during MIS 3

In Fig. 2 the calculated surface temperature evolution is shown over the time period from 64 and 38 kyr BP corresponding to nearly the complete MIS 3. MIS 3 is characterized by various abrupt temperature changes with amplitudes of up to 15 °C (in about 200 yr). A typical mean rate of the temperature change at the beginning of DO events was 0.5±0.1 °C/decade (Table1, Fig. 3). However, maximum temperature rates are about 1 °C/decade. The amplitude of the temperature changes attributed to the different DO events are marked in Fig. 2 and listed in Table 1 and correspond to the integral of the curves in Fig. 3. For the further discussion we distinguish three sequences: (i) DO 12–9, (ii) DO 14–13, (iii) DO 17–15. All three sequences have in common that peak temperatures were high for the first event and were monotonically decreasing for subsequent ones. DO 12 and 17 were preceded by H-events 5 and 6, respectively [40,13]. Event H-5.2, before DO 14, cannot clearly be associated with a H-event, but some sediment proxies as well as sea level changes show H-like behaviour [41,42,13]. However, while DO events

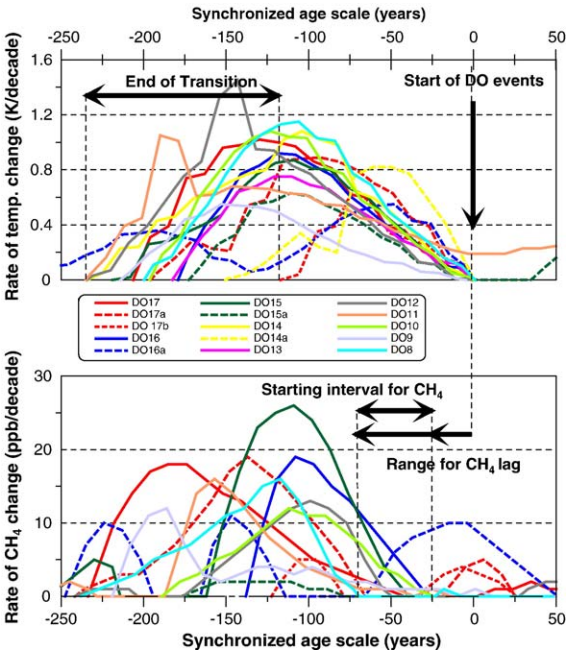

Fig. 3. Rates of change in temperature (top panel) and in methane (bottom panel) for all DO events investigated synchronized to a common time scale. Temperature rates are calculated using the scenario three (see Appendix A). Methane rates are based on a splined version of the NorthGRIP methane data. The spline-data difference is within the measurement uncertainty. The initiation of temperature increase for every DO event is shifted to the year zero. Note that due to very scarce data the methane rates were not calculated for the events DO 13 and DO 14. The length of temperature and methane increase can be retrieved for every single DO event from the time interval of positive rates. Furthermore, the timing between temperature and methane increase can be evaluated. Based on this detailed study, methane lags temperature in the range of 25 to 70 yr with an uncertainty of 25 yr due to the data resolution.

12–9 started with a large event followed by three smaller events, the sequence of DO 14–13 was characterized by a very long and stable warm phase (~2500 yr) followed by a 2000-yr period of intermediate temperatures and a very short cold interval before DO 13 started. The sequence of DO 17–15 was extremely unstable with a characteristic time scale of 400 yr and an amplitude of 7–12 °C. In this time window, all events show a more or less pronounced second temperature peak (labelled with a in the δ^{18}O record of Fig. 2). These events are rather short, e.g., DO 17 (duration = 400 yr, from one cold phase to the next), DO 16 (300 yr), and DO 15a (200 yr), with warm phases of only a few decades. Nevertheless, the first DO events of each cycle, DO events 12, 14 and 17, which are preceded by H-events, show roughly the same temperature change of about 12 °C. The 12.5 °C temperature shift of DO 12 is in agreement with a 12 °C change determined with the combined use of δ^{15}N and δ^{40}Ar measurements on the GRIP ice core [11]. Interestingly, the largest temperature change is not observed for one of the long events, but for DO 11 with a 15±3 °C temperature increase, albeit with a slower rise (580 yr from start to top of peak).

3.2. The $\delta^{18}O_{ice}$ to temperature relationship during MIS 3

Boyle [18] related the shift of the δ^{18}O–T relationship in Greenland ice over the LGM–Holocene transition to changes of tropical sea surface temperatures (SST) in the Atlantic. Changes of the source temperature influence the intercept of the δ^{18}O–T relationship but not the slope (Fig. 4). The simultaneous change of both, the site and the source temperature, results in an apparently smaller slope of δ^{18}O–T relationship. Such calculations were made for the LGM–Holocene transition where the source temperatures were about 4–8 °C cooler than at present [43,44]. The present data permit to test this relationship for stadial–interstadial transitions. In Fig. 4 $\delta^{18}O_{ice}$ corrected for changes of the oxygen isotopic composition of seawater, is plotted versus the isotope calibrated temperature. Our data suggest a similar behaviour of the δ^{18}O–T relationship during stadial–interstadial transitions as between LGM and Holocene. There is a good linear (R^2 = 0.83, geometric mean regression) relationship between δ^{18}O and temperature with a slope of (0.41 ± 0.05) ‰/K which is slightly higher than half the present day spatial slope, corresponding to the values obtained by borehole temperature calibrations [16,45] for the last glacial to interglacial transition. A source temperature change leads to a shift of the line representing the modern δ^{18}O–T relationship parallel to the horizontal axis in Fig. 4.

$\delta^{18}O_{ice}$ does not depend on the mean annual temperature but on the precipitation weighted temperature. Since winter-to-summer temperature and precipitation differences are large, seasonality has an impact on the isotopic composition of the snow [46,47]. The glacial decrease in winter precipitation, predicted by isotope models [17], leads to a $\delta^{18}O_{ice}$ that is much higher than one would expect from the site temperature change alone. This results in a shift of the modern δ^{18}O–T curve parallel to the vertical axis of Fig. 4. Thus seasonality variations can either compensate or amplify the effects of a changing source temperature on the δ^{18}O–T relation. For example, a lowering of the $\delta^{18}O_{ice}$ stadial–interstadial change by 3–4‰ due to an increase of winter precipitation would be consistent with our measurements when constant source temperatures were

Table 1
Rates of changes at the onset of DO events, Δage and Δdepth

DO	Δ*T* Mean (°C) [a]	Uncertainty [b]	Δ*t* (yr) [c]	Rate of change (°C/decade) [d]	ΔCH_4 [a] (ppb)	Rate of change (ppb/°C) [d]	Δage (yr)	Δdepth (m) [e]
9	9 [f]	+3; −6	216	0.28	78	8.7	1067	17.5
10	11.5	+3; −6	198	0.58	88	7.7	1129	17
11	15	+3; −6	357	0.42	112	7.5	1166	16
12	12.5 [g]	+3; −6	236	0.53	88	7.0	1052	13.5
13	8	+3; −6	183	0.44	–	–	834	13
14	12.5	+3; −6	235	0.53	117	9.4	984	12
15	10	+3; −6	215	0.47	163	16.3	923	13
16	9	+3; −6	180	0.5	121	13.4	668	11.5
17	12	+3; −6	206	0.58	185	15.4	1038	11.5

[a] Temperature and CH_4 amplitude change from start to top of DO event, respectively.
[b] A range of uncertainty from (+3 to −6) °C is given. From $\delta^{15}N$ measurements a symmetric uncertainty of ±3 °C would be applicable. The extended range results from effects not investigated in this study, mainly addressing the potential of a rapidly changing convective zone in parallel to the DO events (see text for details).
[c] Time from start to top of DO event.
[d] Note that these are mean rates. For methane they can be slightly higher compared to the values derived from Fig. 3 due to data splining within its uncertainty of 10 ppb.
[e] Depth difference between the warming recorded in $\delta^{18}O_{ice}$ and in $\delta^{15}N$.
[f] Note that the temperature increase given here corresponds to a two step increase of three and six degrees. These two steps are separated by about 400 yr.
[g] Prior to the rapid temperature shift for DO 12 a slow but significant temperature increase of several degrees has occurred.

assumed. Hence, the deviation from the hypothetical glacial line in Fig. 4 can be viewed as a linear combination of source temperature changes and changes in the distribution of precipitation throughout the year. If one parameter can be constrained the other can be inferred.

Assuming only minor variations of the seasonal distribution of precipitation, our findings would imply that source temperature changes of about 4–8 °C for single DO events were in phase with site temperature variations on millennial time scales. This agrees with reconstructions from the subtropical North Atlantic where temperature changes of 2–5 °C were found during MIS 3, covarying with Greenland $\delta^{18}O$ of ice cores [44].

On the other hand, it is inconsistent with measurements of the deuterium-excess (representing the source temperature) and the $\delta^{18}O_{ice}$ (representing the site temperature) on the GRIP ice core which are anti-correlated on millennial time scales [19]. This anti-correlation (Greenland cold, source region warm) could be the result of a southward shift of the moisture source during stadials, possibly due to extensive sea ice cover. A consistent explanation of the observed $\delta^{18}O$–*T* relation with such a scenario requires large changes in the seasonality of precipitation between stadials and interstadials. Model simulations indicate such seasonality for the Last Glacial maximum [48] and for the Younger Dryas termination [46]. A shift of winter storm tracks towards Greenland could be responsible for the higher winter precipitation during warm stages compared to cold stages.

3.3. CH_4 and temperature

In parallel to nitrogen isotopes, CH_4 was measured on the NorthGRIP ice for the sequences of DO 12–9 [29] and DO 17–15 (new data). As shown by others before, the correlation between CH_4 and Greenland temperature is extraordinarily strong [30,49,50]. Usually such correlations were done using $\delta^{18}O_{ice}$ as a direct temperature proxy, which is not exactly true as shown above. Furthermore, additional uncertainties in the timing of both records arose from Δage determinations in these prior studies. Here a much more direct comparison is possible, since both, temperature ($\delta^{15}N$) and CH_4, are gas species and were measured along the same cores. Therefore, we can investigate the relative timing of CH_4 and temperature evolution. The timing uncertainty corresponds to the data resolution of about 25 yr during DO increases, whereas elsewhere it is 50–100 yr. Generally we find a good agreement between CH_4 and temperature rises at the onset of the observed DO events (Figs. 2 and 5). A detailed view of the timing of the investigated DO events is given in Fig. 3. The upper part is a compilation of the rate of temperature changes per decade (K/decade) of all DO events matched onto a common time scale from the start of the DO event. Plotted are only the positive temperature

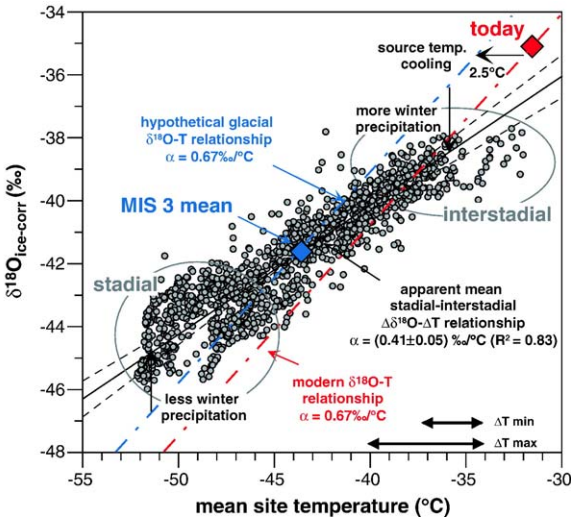

Fig. 4. NorthGRIP $\delta^{18}O_{ice}$ is plotted against the calibrated NorthGRIP temperature (grey dots). $\delta^{18}O_{ice}$ is corrected for changes of the oxygen isotopic composition of seawater. For MIS 3 the Dole effect is small [70] therefore we use the corresponding $\delta^{18}O_{atm}$, since atmospheric $\delta^{18}O_{atm}$ variations reflect changes of oceanic $\delta^{18}O$ but are delayed by about 1500–2500 yr. In particular we use the $\delta^{18}O_{atm}$ measurements from NorthGRIP ($\delta^{18}O_{atm} = \delta^{18}O_{measured} - 2\,\delta^{15}N_{measured}$) shifted 2000 yr toward older ages to correct for this effect. The curve with the modern $\delta^{18}O$–T slope ($\alpha = 0.67‰/°C$) is plotted through the present day NorthGRIP value (red diamond) and through the mean value of our data (MIS 3 mean) (blue diamond). The data do not follow these curves. Offsets can be explained by a linear combination of source temperature changes and changes in the distribution of precipitation throughout the year. The uncertainty for the temperature estimates based on $\delta^{15}N$ is given as minimal and maximal error (black arrows). The minimum error accounts only for the uncertainty of $\delta^{15}N$, whereas the maximum error includes potential rapid changes of the convective zone (see text).

rates corresponding to temperature increases. It is interesting to note that most DO events show very similar temperature increase rates. The lengths of the increasing interval are between 100 to 250 yr, defined as the time interval of positive temperature rates. The start of each single DO event is set to zero years on the time axis with one exception. DO 11 has an extraordinary constant rate of temperature increase during the first 120 yr prior to the sharp increase. Therefore, the starting time was shifted by 120 yr, mainly for clarity reasons in Fig. 3. Hence, the temperature rate for this event is above the zero level in contrast to all other events at zero years.

In the lower part of Fig. 3, the corresponding rates of CH_4 changes (ppb/decade) are given. Methane rates were derived from the spline-smoothed NorthGRIP data. The spline-data difference is well within the data uncertainty of 10 ppv, therefore we expect insignificant influence of the data splining on methane rates for DO events. Note, that there are no high resolution CH_4 values available for DO 13 and DO 14. As can be seen, the timing of CH_4 rises generally lags the rises in temperature by 25 to 70 yr with an uncertainty of about 25 yr in good agreement with the estimate of Severinghaus and Brook [10] for the end of the last glacial period. There are exceptions for the short events, i.e., DO 17b, DO 16a and DO 15a. Furthermore, the CH_4 increase is generally shorter than the temperature increase. The lag occurring at the mid-slope (at maximum of CH_4 changing rates) of DO event is less pronounced than at the onset.

The correlation between CH_4 and the calibrated temperature record is higher ($R^2 = 0.82$) than that between CH_4 and $\delta^{18}O_{ice}$ ($R^2 = 0.74$) for the sequence DO 12–9. This is most probably because $\delta^{18}O_{ice}$ includes other influences than temperature (local seasonal precipitation distribution and/or source region movements) as discussed above. For the sequence DO 17–15, however, the correlation coefficient using the calibrated temperature is slightly lower compared to the direct $\delta^{18}O_{ice}$–CH_4 correlation ($R^2 = 0.72$ and 0.77, respectively). The slope (rate of change in Table 1) of the CH_4 to temperature dependency is changing substantially for the different periods. It is higher for DO 17–15 than for the period DO 12–9 (Table 1). This is in agreement with previous studies [50,29] suggesting

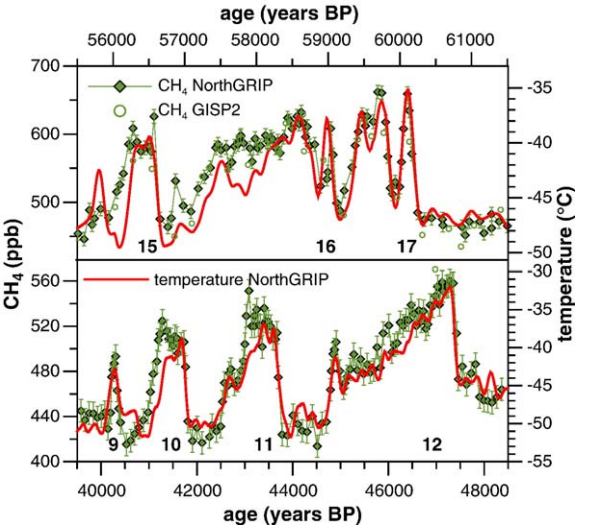

Fig. 5. Calibrated NorthGRIP temperature evolution (red line) compared to atmospheric methane concentration measurements (CH_4) from the NorthGRIP (Flückiger et al. [29] and new measurements) and the GISP2 [50] ice cores (green symbols and lines). The data are plotted on the GRIP2001/ss09sea [39,26] age scale. (Top panel): Sequence of DO 17–15, 61.5 to 55.5 kyr BP. (Bottom panel): Sequence of DO 12–9, 48.5 to 39.5 kyr BP. Note that the scales of temperature and CH_4 are chosen differently for the two panels because the CH_4 amplitudes are higher for DO 17–15 than for DO 12–9 (Fig. 2).

a possible link of the CH_4 amplitudes with the summer insolation of tropical to mid-northern latitudes.

The main preanthropogenic CH_4 sources were wetlands, mainly located in the tropical regions and the northern mid-latitudes [49–51]. CH_4 emissions are influenced by changes in precipitation and temperature via the extent and productivity of wetland ecosystems [52]. The CH_4 variations in parallel to DO events are thought to be caused by source changes in the tropical and/or the northern mid-latitudes [31,53,29]. Rapid and large releases of methane are most likely not the origin of the observed methane increases during DO events as studied by Brook et al., [54]. Contributions from decadal to centennial thawing of permafrost regions can, however, not be excluded for these events [55].

A detailed comparison of CH_4 with temperature for the two DO sequences 12–9 and 17–15 is shown in Fig. 5. Note that the scales of temperature and CH_4 are chosen differently for the two panels in Fig. 5, since the CH_4 amplitudes are higher for DO 17–15 than for DO 12–9 [50,29]. The presented DO events allow us to focus on the submillennial variability of CH_4 and Greenland temperature during the glacial period, since the timing uncertainty is <100 yr over the entire record. For DO 17, 16, 12, and 11 even small submillennial temperature excursions have a clear counterpart in the CH_4 record. During the other presented DO events the correlation is less pronounced but still substantial. Similar features can be seen in the CH_4 record of the Greenland ice core GISP2 [31,30] which is matched to the NorthGRIP (ss09sea) time scale using NorthGRIP CH_4. There is only one temperature peak that has no counterpart in CH_4 (DO 15a), which most probably was missed due to an insufficient sample resolution in both the CH_4 and the $\delta^{15}N$ records. The most obvious discrepancies between CH_4 and temperature can be seen at the end of DO 10 and 15, where CH_4 decreases more slowly than temperature. Three possible explanations are offered for this mismatch. First, other factors than temperature controlling wetland CH_4 emissions such as precipitation, water tables, vegetation changes could have remained unchanged or have not reacted immediately to temperature changes at the end of these DO events. Hence the wetland CH_4 emissions drop slower. Second, the Greenland temperature reconstruction is believed to be hemispheric in extent in agreement with recent modelling results [7]. However, precipitation changes or different decrease rates between northern and tropical temperature that could result in a lag of $\sim$100 yr at the end of the decrease cannot be excluded. In this case tropical CH_4 sources behave differently from the northern ones. Third, the accumulation rate used to force the model could be in error for certain periods resulting in a different reconstructed temperature record for those time intervals. The question remains why not all DO events show this behaviour. Therefore, DO 10 and DO 15 should definitely be investigated further, e.g., by measuring the CH_4 stable isotope compositions, in order to constrain the origin of the CH_4 sources active during MIS 3.

4. Conclusions

The abrupt temperature changes associated with the 9 consecutive DO events 9–17 are in the range of 8 to 15 °C. The 12.5 °C temperature change of DO 12 is consistent with an earlier reconstruction of 12 °C on ice from a different site and using a different method [11]. This finding also supports earlier results from DO 19 that showed a 16 °C temperature change in GRIP as well as in NorthGRIP [9,12].

Furthermore, a detailed comparison of the temperature evolution with measurements of the atmospheric CH_4 concentration shows that CH_4 and temperature rise at the onset of DO events are nearly in phase. A small lag of 25 to 70 yr with an uncertainty of 25 yr was observed for methane compared to temperature. There is also a good correlation between both parameters on millennial and sub-millennial time scales. This is strong evidence that even sub-millennial scale signals registered in Greenland represent probably hemispheric signatures.

Finally, we can relate the discrepancy between the modern and the glacial $\delta^{18}O_{ice}$–T relationship to a combination of source temperature changes and changes in the annual distribution of precipitation. We conclude that on millennial time scales rapid temperature changes were most probably in phase with reorganisations of the seasonal precipitation distribution (lower temperature, less winter precipitation) resulting in a reduction of the apparent slope of the $\delta^{18}O$–T relationship compared to the present day value. If changes of the source temperatures can be constrained, for example by deuterium excess measurements [19], it may become possible to quantify the strength of the seasonality changes.

Acknowledgements

We would like to thank two anonymous reviewers for their extensive comments and suggestions that improved this manuscript considerably. We thank Gregor Hausammann for his support during the CH_4 measurements.

This work, as part of the NorthGRIP Project, was supported by the University of Bern and the Swiss National Science Foundation. The NorthGRIP Project is coordinated by the Department of Geophysics at the Niels Bohr Institute for Astronomy, Physics and Geophysics, University of Copenhagen. It is supported by Funding Agencies in Denmark (SHF), Belgium (FNRS-CFB), France (IPEV and INSU/CNRS), Germany (AWI), Iceland (RannIs), Japan (MEXT), Sweden (SPRS), Switzerland (SNF) and the United States of America (NSF, Office of Polar Programs).

Appendix A

A.1. Approach 1

The three tuneable input parameters of the model are the surface temperature, the accumulation rate and the sum of convective and non-diffusive zone z_s. Accumulation rates and ice thinning (strain) are prescribed by the ice flow dating model of the core [56]. Hence when using a certain age scale, the accumulation rate is fixed and the remaining tuneable parameters are the temperature and z_s. In this study we use the ss09sea age scale, which is an improved GRIP age scale [39] adopted to NorthGRIP [26], and the ss06 age scale, which is currently the best NorthGRIP age scale available.

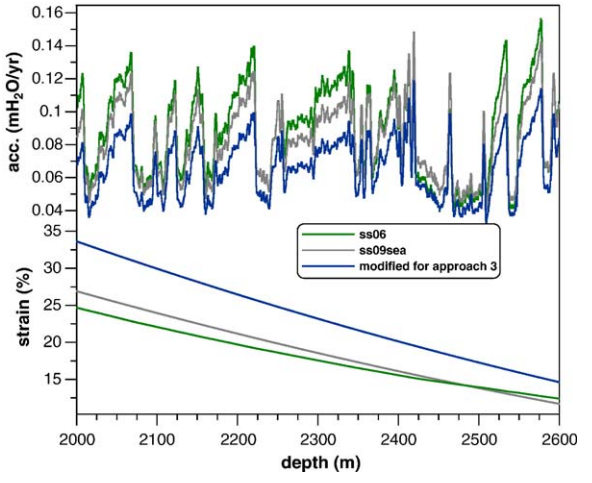

Fig. 6. Comparison of the parameterisations of the accumulation rate and the ice thinning (strain) of the NorthGRIP age scales ss09sea (grey line) and ss06 (green line). Additionally modified accumulation rate scenario (ss09sea−20%) and strain (ss09sea+25%) used for the calculations in approach 3 are plotted (blue line). Note that the product of accumulation rate times strain remains constant, i.e., retained time scale for both ss09 scenarios (grey and blue line). (For interpretation of the references to colour in this figure legend, the reader is referred to the web version of this article.)

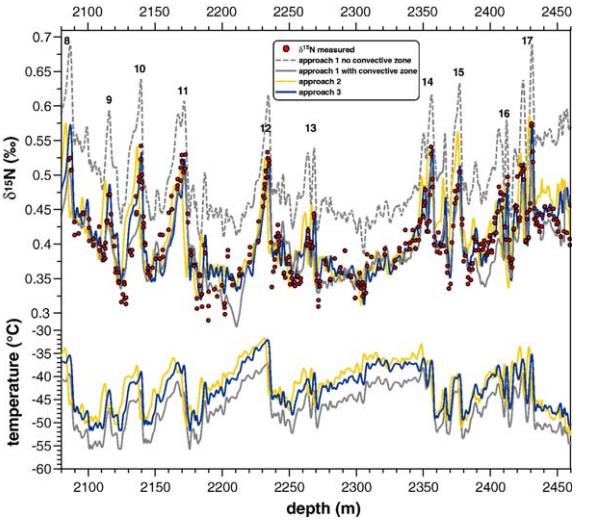

Fig. 7. Top panel: $\delta^{15}N$ measurements (red dots) and firn model calculations versus ice depth. Bottom panel: Surface temperature evolution used as model input. The different approaches are described in the text. (For interpretation of the references to colour in this figure legend, the reader is referred to the web version of this article.)

Accumulation rate and thinning show relative differences of up to about 10% (Fig. 6).

We use $T_s=(\delta^{18}O_{ice}+35.1‰)\alpha^{-1}+241.6$ K, where α is the $\delta^{18}O_{ice}$ to temperature sensitivity. We ran the model for different values of α (α=0.30, 0.35, 0.40, 0.45, 0.50‰/K). Since, α can change from one DO event to another it is not possible to find a constant value for α that matches the data for the entire time period. Hence, data and model should be fitted for short time periods of about 2000 yr only. The best correlation between the model and the $\delta^{15}N$ data for a 2000-yr time window was searched by varying z_s and α linearly between the different calculated scenarios. Thereafter the time window was shifted by 250 yr and the procedure was repeated, until all DO events were scanned. In order to obtain an error estimate for α and z_s, we tested the sensitivity of the fitting procedure to errors of the $\delta^{15}N$ measurements (Monte Carlo simulations). For every time window 200 fits were performed. For each fitting procedure the $\delta^{15}N$ data were randomly modified by a Gaussian distributed standard error of ±0.02‰. The model matches the data within this error range. The result of this fitting procedure can be seen in Fig. 7 (grey line).

The timing as well as the amplitudes of abrupt changes match excellently. However, modelled $\delta^{15}N$ values assuming $z_s\equiv 0$ (dashed grey line), are significantly higher (0.07–0.1‰) than the measurements. In order to explain an offset, $\Delta\delta=\delta_{model}-\delta_{data}$ of 0.1‰, a reduction of the diffusive column height by either an

increase of the convective zone near the surface, or an increase of the non-diffusive zone near the bottom of the firn, or a combination of both, of 20 m would be needed. For present-day conditions at Greenland, convective zones are non-existent or rather small (<5 m) [57,58]. However, during glacial times convective zones could be significantly larger, e.g., due to increased wind pumping of lower accumulation rates associated with lower temperatures [59]. The Antarctic sites of Dome Fuji and Vostok have convective zones between 8–12 m. Severinghaus et al. [60] reported an Antarctic site were a deep (20 m) convective zone exists. As a result of the lack of winter accumulation deep cracks are formed in the firn. But, considering the higher accumulation and temperatures in Greenland, convective zones of 20 m or more are very unlikely, even during glacials. A disagreement between data and model during glacials has been observed for other ice cores as well. Measured δ^{15}N values at nearly all Antarctic sites are lower as predicted by the models. Additionally, Schwander et al. [36] found a similar behaviour for the Greenland cores GRIP and GISP2. On the other hand, two newer studies were able to model δ^{15}N properly during certain time frames of the GISP2 and GRIP cores [22,11] assuming a small convective zone of 2 to 5m.

An independent verification of the model findings can be done using the Δdepth. The Δdepth is the depth difference between an event recorded in the gas phase, as δ^{15}N peak, and in the ice phase, as $\delta^{18}O_{ice}$ peak. It depends on the lock in depth (LID) at the time of bubble inclusion, and on the thinning of the ice with depth. From the age scale model we know the thinning function. Hence we are able to recalculate past LID. LID determined by the firn-densification model [34] and the LID recalculated from Δdepth measurements show a mean difference of five meters (Fig. 8, grey dots and line). This is actually an additional indication that approach 1 is incorrect like approach 2 and supports approach 3 (see below).

If the offset, $\Delta\delta$, is interpreted as a convective zone, we have to correct the modelled δ^{15}N data. The gravitational enrichment is reduced by the offset. This leads to a perfect matching of model and data (Fig. 7, grey line). However, by doing this a reduced ΔT has to be used for the thermal diffusion effect, since at a depth of 10–20 m, corresponding to z_s (Fig. 8), the surface temperature signal is smoothed, therefore reducing the thermal signal recorded in the nitrogen isotopes. This is due to the fact that heat transfer by air movement is not able to level out the firn temperature to a depth of 10 m or more [59]. The result of this correction is a reduction of the modelled

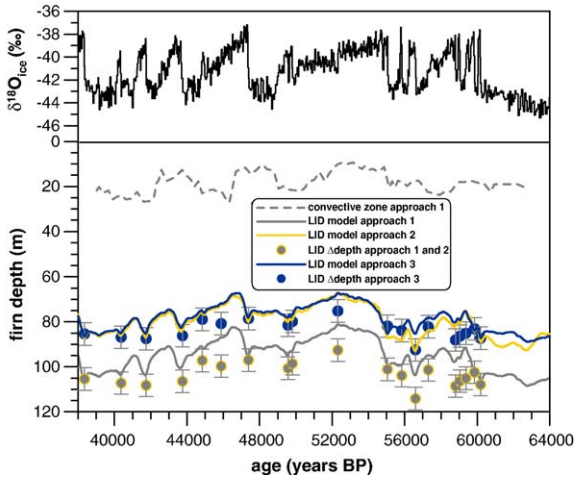

Fig. 8. Top panel: $\delta^{18}O_{ice}$ of NorthGRIP on the ss09sea age scale. Bottom panel: Lock in depths (LID) for the different approaches determined by the firn densification model (solid lines), and calculated from Δdepth measurements using the ice thinning function (dots). The dashed line shows the size of the convective zone as calculated in approach 1.

δ^{15}N values, as shown in Fig. 7. Short DO events are more affected by the smoothing process than longer ones. Though the depth of the convective zone accounts for only about 10–20% of the porous firn column, the temperature gradient is reduced by as much as 40% [36]. In order to match the measured δ^{15}N data with the model, we would have to increase the surface temperature changes by up to 40% accordingly. Consequently, temperature changes for short events would become larger than for the long events. Such a scenario is very unlikely. All the more, Landais et al. [11] found a 12 °C temperature change for DO 12 on the GRIP ice core, using the $\delta^{15}N_{excess}$ method, which agrees nicely with the value we found in the uncorrected temperature scenario. An alternative explanation of the offset could be by an enlarged non-diffusive zone instead of a convective zone. A non-diffusive zone can be caused by inhomogeneities in the firn structure, due to different densities of summer and winter layers, as well as by crusts and melt-layers. Dense layers can cause a complete sealing of the firn column at depths far above the level where the mean firn diffusivity reaches zero values. Such layers would reduce the DCH. The model does account for a non-diffusive zone using empirical relations between firn density, open porosity, tortuosity and diffusivity [57,61,36]. Possible effects of layering are not incorporated in the model. However, for glacial conditions an increased layering is very unlikely, since temperatures were much colder, accumulation

rates were lower and winter precipitation was nearly absent [17]. Such conditions lead to a more homogeneous density structure of the firn, which contradicts the scenario of a larger non-diffusive zone.

A.2. Approach 2

From our calculations for approach 1 we found a clear anti-correlation between the offset, $\Delta\delta$ or z_s and α (not shown). To calculate the temperature for approach 1, we assumed a linear relation of temperature and $\delta^{18}O_{ice}$: $T=\delta^{18}O_{ice}\,\alpha^{-1}+\beta$, where β was constrained by recent values for $\delta^{18}O_{ice}$ and temperature. The anti-correlation of $\Delta\delta$ or z_s and α could be a result of this constraint. Hence, another way to circumvent the offset could be a shift in the absolute temperature. A 3.5 °C mean temperature increase, reduces the DCH by 10 m and $\delta^{15}N$ by 0.05‰, respectively. Thus, the $\Delta\delta$ or z_s can be translated into an additional temperature shift. As a result of this offset corrected temperature scenario (Fig. 7, dark grey line) the vertical offset indeed disappears, but now we have a disagreement in the timing between model and data. This mismatch is best seen for DO 9 to 12 in Fig. 7. Even more convincing for this timing problem are the Δdepth calculations (Fig. 8), which disagree completely for approach 2.

Hence it is not possible to find a realistic temperature scenario with our model by using the accumulation rates of the ss09sea age scale model. The same calculation can be done with the ss06 age scale with the same conclusion. Therefore, possibly the parameterisation of the accumulation rates with $\delta^{18}O_{ice}$ is wrong for the observed time period.

A.3. Approach 3

The accumulation rate depends on temperature. In the parameterisation used in the age scale model, the accumulation rate is calculated from Approach 2: (corrected by the changing $\delta^{18}O$ of seawater), using an empirical relation based on measurements form various sites in Greenland [63,62]. This relation describes recent climatic conditions. Hence, using the same relation for glacial conditions can only give a rough estimate of the accumulation rates at these times. Accumulation rates could likely be different. But they cannot be varied arbitrarily, since otherwise the age scale of the ice core, which is constrained independently, changes. There are two principal ways to avoid age scale conflicts: (1) to change both, the accumulation rate and the ice thinning function, since the age scale depends only on the product of accumulation and thinning and (2) to change only the slope of the accumulation to $\delta^{18}O$ dependency, but not the mean accumulation over a certain time period. Increasing the slope then corresponds to higher accumulation during warm times and lower accumulation during cold times. Thus, it will stretch and compress the age scale for short time windows, but it will not affect it on long scales. The consequences of the latter accumulation modifications are documented in Fig. 9. Three different accumulation scenarios (0.5 × slope, 1 × slope, 2 × slope) are compared. The age scale is constrained at 35 and at 65 kyr BP. The temperature scenario is calculated from $\delta^{18}O_{ice}$ using $\alpha=0.4$‰/K. A reduction of the slope causes a stretching of the cold phases and a compression of the warm phases. The higher the slope, the longer the warm phases and the shorter the cold phases become. Hence, we can tune the length of the events if necessary. For example, the slight disagreement between data and model at the end of DO 10 (Figs. 5 and 7) could probably be solved by reducing the slope during this time interval. However, the offset in $\delta^{15}N$ between model and data remains nearly unchanged (about 0.1‰) for (2).

The disagreement of the LID for approach 2 (Fig. 7) between the model calculation and the Δdepth reconstruction is about 20% to 25% over the entire time period. The LID calculated from Δdepth is directly proportional to the thinning function. Hence

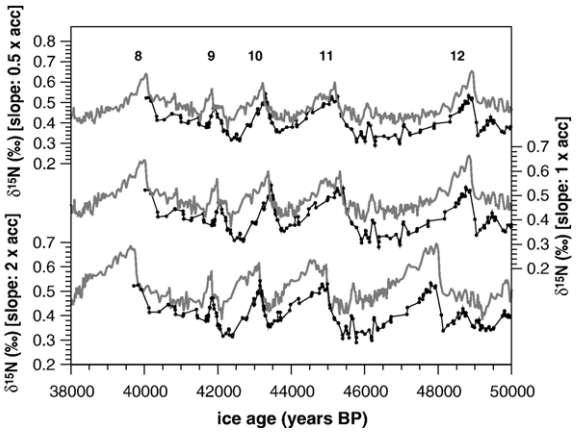

Fig. 9. A comparison of three different accumulation scenarios (0.5 × slope, 1 × slope, 2 × slope) covering DO 8 to 12. Model output is plotted as grey lines, measurements as black lines and dots. The age scale was constrained at 35 kyr BP and at 65 kyr BP using given depths. The temperature scenario was calculated from $\delta^{18}O_{ice}$ using $\alpha=0.4$‰/K. It can be seen that the higher the slope is, the longer the warm phases and the shorter the cold phases become.

for (1), we have to reduce the ice thinning by about 25% to obtain a better agreement. In order to conserve the age scale, the accumulation rate must be adjusted accordingly. Results are shown in Fig. 7 (black line). Accumulation is reduced by 20% compared to ss09sea (Fig. 6, black line), this reduction is consistent with findings of Cuffey and Clow [38] who obtained lower accumulation rates for GISP2 compared to GRIP and NorthGRIP during the glacial times. The temperature evolution bases on the Monte Carlo calculations from approach 1, but the absolute temperature is corrected by 4 °C towards higher values. This leads to a 20% lower gravitational enrichment that requires some readjustments on the temperature evolution scenario of approach 1. This has been done by minimizing the square root deviations between model and data. This scenario leads to an excellent agreement for both, the amplitudes as well as the timing of the events. Model matches the data within the analytical error range of 0.02‰. As expected, the LID of the model and the calculations by the Δdepth correspond within the uncertainty range of the Δdepth determination. These calculations are made under the assumption that the convective zone was zero.

A.4. Additional information from oxygen isotopes

Parallel to $\delta^{15}N$ and $\delta^{40}Ar$ we determined $\delta^{18}O$ of O_2 on the NorthGRIP ice samples. From these measurements we can calculate the atmospheric oxygen isotope composition $\delta^{18}O_{atm}$, which can be compared with measurements from other ice cores from both hemispheres, since O_2 is well mixed in the atmosphere [68]. $\delta^{18}O_{atm}$ is usually obtained using $\delta^{15}N$ to correct for gravitational effects. According to Eq. (1) the gravitational enrichment of $\delta^{18}O$ is two times the enrichment of $\delta^{15}N$ ($\delta^{18}O_{atm}=\delta^{18}O-2\cdot\delta^{15}N$). This calculation underestimates $\delta^{18}O_{atm}$ at the time of rapid temperature changes, since the ratio of thermal diffusion factors of $\delta^{18}O$ and $\delta^{15}N$ is only 1.6, which is slightly lower than the effect of gravitation. However, the maximum shift associated with this approximation is about twice the analytical uncertainty of our measurements of ±0.05‰, much less than the signal variations. The resulting $\delta^{18}O_{atm}$ record matches Vostok [64–67] and GISP2 [68] $\delta^{18}O_{atm}$ data (Fig. 10) when the NorthGRIP age scale is shifted by 2000 ±500 yr towards younger ages. Note that the data are plotted on different age scales (NorthGRIP ss09sea, Vostok GT4 [66], and GISP2 [69]) in Fig. 10. These results are an independent constraint of the North-

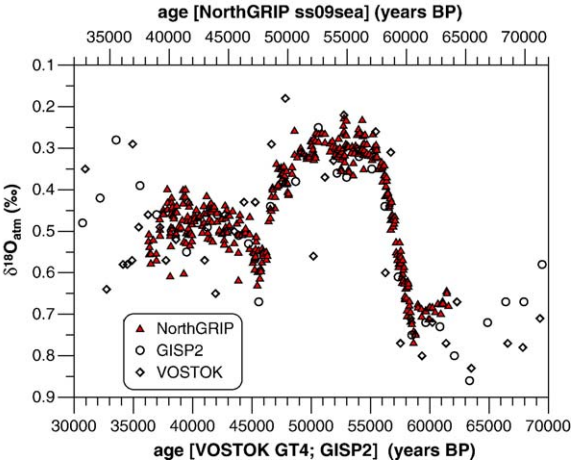

Fig. 10. Atmospheric oxygen data $\delta^{18}O_{atm}$ from NorthGRIP (filled triangles) is plotted together with $\delta^{18}O_{atm}$ from the GISP2 (open circles) [68] and Vostok (open diamonds) [64–66] ice cores. The NorthGRIP $\delta^{18}O$ measurements were corrected for gravitational fractionation using $\delta^{15}N$. The different data are plotted on their individual age scales. The different age scales are offset, but not the $\delta^{18}O_{atm}$ values. After shifting the North GRIP ss09sea age scale by 2000±500 yr, the data match within an error range of ±0.05‰.

GRIP ss09sea age scale. This shift of 2000 yr has no impact on the conclusions of this paper, because it is more or less constant over the entire MIS 3.

References

[1] W. Dansgaard, S.J. Johnsen, H.B. Clausen, D. Dahl-Jensen, N.S. Gundestrup, C.U. Hammer, C.S. Hvidberg, J.P. Steffensen, A.E. Sveinbjörnsdottir, J. Jouzel, G. Bond, Evidence for general instability of past climate from a 250 kyr ice-core record, Nature 364 (1993) 218–220.

[2] Y.J. Wang, H. Cheng, R.L. Edwards, Z.S. An, J.Y. Wu, C.-C. Shen, J.A. Dorale, A high-resolution absolute-dated Late Pleistocene monsoon record from Hulu Cave, China, Science 294 (2001) 2345–2348.

[3] M.A. Altabet, M.J. Higginson, D.W. Murray, The effect of millenial-scale changes in Arabian Sea denitrification on atmospheric CO_2, Nature 415 (2002) 159–162.

[4] G. Bond, W. Broecker, S. Johnsen, J. McManus, L. Labeyrie, J. Jouzel, G. Bonani, Correlations between climate records from North Atlantic sediments and Greenland ice, Nature 365 (1993) 143–147.

[5] N.J. Shackleton, M.A. Hall, E. Vincent, Phase relationships between millenial-scale events 64,000–24,000 years ago, Paleoceanography 15 (2000) 565–569.

[6] T.F. Stocker, O. Marchal, Abrupt climate change in the computer: is it real? Proceeding of the US National Academy of Science, vol. 97, 4, 2000, pp. 1362–1365.

[7] R. Knutti, J. Flückiger, T.F. Stocker, A. Timmermann, Strong hemispheric coupling of glacial climate through freshwater discharge and ocean circulation, Nature 430 (2004) 851–856.

[8] W.S. Broecker, Thermohaline circulation: the Achilles heel of climate system, Science 278 (1997) 1582–1588.

[9] C. Lang, M. Leuenberger, J. Schwander, S. Johnsen, 16 °C rapid temperature variation in central Greenland 70,000 years ago, Science 286 (1999) 934–937.
[10] J.P. Severinghaus, E.J. Brook, Abrupt climate change at the end of the last glacial period inferred from trapped air in polar ice, Science 286 (1999) 930–934.
[11] A. Landais, N. Caillon, C. Goujon, A. Grachev, J.M. Barnola, J. Chappellaz, J. Jouzel, V. Masson-Delmotte, M. Leuenberger, Quantification of rapid temperature change during DO event 12 and phasing with methane inferred from air isotopic measurements, Earth and Planetary Science Letters 225 (2004) 221–232.
[12] A. Landais, J.M. Barnola, V. Masson-Delmotte, J. Jouzel, J. Chappellaz, N. Caillon, C. Huber, M. Leuenberger, S.J. Johnsen, A continuous record of temperature evolution over a whole sequence of Dansgaard–Oeschger during Marine Isotope Stage 4 (76 to 62 kyr BP), Geophysical Research Letters 31 (L22211) (2004), doi:10.1029/2004GL021193.
[13] S.R. Hemming, Heinrich Events: massive Late Pleistocene detritus layers of the North Atlantic and their global climate imprint, Geophysical Research Letters 42 (1) (2004) RG1005, doi:10.1029/2003RG000128.
[14] W. Dansgaard, Stable isotopes in precipitation, Tellus 16 (1964) 436–468.
[15] K.M. Cuffey, R.B. Alley, P.M. Grootes, J.M. Bolzan, S. Anandakrishnan, Calibration of the $\delta^{18}O$ isotopic paleothermometer for central Greenland, using borehole temperatures, Journal of Glaciology 40 (135) (1994) 341–349.
[16] S. Johnsen, D. Dahl-Jensen, W. Dansgaard, N. Gundestrup, Greenland palaeotemperatures derived from GRIP bore hole temperature and ice core isotope profiles, Tellus 47B (1995) 624–629.
[17] M. Werner, M. Heimann, G. Hoffmann, Isotopic composition and origin of polar precipitation in present and glacial climate simulations, Tellus 53B (2001) 53–71.
[18] E.A. Boyle, Cool tropical temperatures shift the global $\delta^{18}O$–T relationship: an explanation for the ice core $\delta^{18}O$–borehole thermometry conflict? Geophysical Research Letters 3 (1997) 273–276.
[19] V. Masson-Delmotte, J. Jouzel, A. Landais, M. Stievenard, S.J. Johnsen, J.W.C. White, M. Werner, A. Sveinbjornsdottir, K. Fuhrer, GRIP deuterium excess reveals rapid and orbital-scale changes in Greenland moisture origin, Science 309 (2005) 118–121.
[20] M.C. Leuenberger, C. Lang, J. Schwander, Delta ^{15}N measurements as a calibration tool for the paleothermometer and gas-ice age differences: a case study for the 8200 B.P. event on GRIP ice, Journal of Geophysical Research 104 (D18) (1999) 22163–22170.
[21] J.P. Severinghaus, A. Grachev, B. Luz, N. Caillon, A method for precise measurement of argon 40/36 and krypton/argon ratios in trapped air in polar ice with applications to past firn thickness and abrupt climate change in Greenland and at Siple Dome, Antarctica, Geochimica et Cosmochimica Acta 67 (3) (2003) 325–343.
[22] C. Goujon, J.-M. Barnola, C. Ritz, Modeling the densification of polar firn including heat diffusion: application to close-off characteristics and gas isotope fractionation for Antarctic and Greenland sites, Journal of Geophysical Research 108 (2003), doi:10.1029/2002JD003319.
[23] A. Mariotti, Atmospheric nitrogen is a reliable standard for natural ^{15}N abundance measurements, Nature 303 (1983) 685–687.
[24] J.P. Severinghaus, T. Sowers, E.J. Brook, R.B. Alley, M.L. Bender, Timing of abrupt climate change at the end of the Younger Dryas interval from thermally fractionated gases in polar ice, Nature 391 (1998) 141–146.
[25] A. Landais, V. Masson-Delmotte, J. Jouzel, D. Raynaud, S. Johnsen, C. Huber, M. Leuenberger, J. Schwander, B. Minster, The glacial inception as recorded in the NorthGRIP Greenland ice core: timing, structure and associated abrupt temperature changes, Climate Dynamics (2005) 1–12, doi:10.1007/s00382-005-0063-y.
[26] NorthGRIP Members, High resolution Climate Record of the Northern Hemisphere reaching into the last Glacial Interglacial Period, Nature 431 (2004).
[27] C. Huber, M. Leuenberger, O. Zumbrunnen, Continuous extraction of trapped air from bubble ice or water for on-line determination of isotope ratios, Analytical Chemistry 75 (10) (2003) 2324–2332.
[28] C. Huber, M. Leuenberger, Measurements of isotope and elemental ratios of air from polar ice with a new on-line extraction method, Geochemistry Geophysics Geosystems 5 (10) (2004) Q10002, doi:10.1029/2004GC000766.
[29] J. Flückiger, T. Blunier, B. Stauffer, J. Chappellaz, R. Spahni, K. Kawamura, J. Schwander, T.F. Stocker, D. Dahl-Jensen, N_2O and CH_4 variations during the last glacial epoch: insight into global processes, Global Biogeochemical Cycles GB 1020 (2004), doi:10.1029/2003GB002122.
[30] T. Blunier, E. Brook, Timing of millennial-scale climate change in Antarctica and Greenland during the last glacial period, Science 291 (2001) 109–112.
[31] E.J. Brook, S. Harder, J. Severinghaus, M. Bender, Atmospheric methane and millennial-scale climate change, in: P.U. Clark, R.S. Webb, L.D. Keigwin (Eds.), Mechanisms of Global Climate Change at Millennial Time Scale, Geophysical Monograph, vol. 112, AGU, Washington, DC, 1999, pp. 165–175.
[32] H. Craig, Y. Horibe, T. Sowers, Gravitational separation of gases and isotopes in polar ice caps, Science 242 (1988) 1675–1678.
[33] J. Schwander, The transformation of snow to ice and the occlusion of gases, in: H. Oeschger, C.C. Langway Jr. (Eds.), The Environmental Record in Glaciers and Ice Sheets, John Wiley, New York, 1989, pp. 53–67.
[34] A. Grachev, J.P. Severinghaus, Laboratory determination of thermal diffusion constants for $^{29}N_2/^{28}N_2$ in air at temperatures from −60 to 0 °C for reconstruction of magnitudes of abrupt climate changes using the ice core fossil–air paleothermometer, Geochimica et Cosmochimica Acta 67 (3) (2003) 345–360.
[35] W.S.B. Paterson, The Physics of Glaciers, Pergamon, Tarrytown, N.Y., 1994, 480 pp.
[36] J. Schwander, T. Sowers, J.-M. Barnola, T. Blunier, B. Malaizé, T. Fuchs, Age scale of the air in the summit ice: implication for glacial–interglacial temperature change, Journal of Geophysical Research 102 (D16) (1997) 19483–19494.
[37] A. Grachev, J.P. Severinghaus, Determining the thermal diffusion factor for $^{40}Ar/^{36}Ar$ in air to aid paleoreconstruction of abrupt climate change, The Journal of Physical Chemistry. A 107 (2003) 4636–4642.
[38] K.M. Cuffey, G.D. Clow, Temperature, accumulation, and ice sheet elevation in central Greenland through the last deglaciation transition, Journal of Geophysical Research 102 (12) (1997) 26383–26396.
[39] S.J. Johnsen, D. Dahl-Jensen, N. Gundestrup, J.P. Steffensen, H. B. Clausen, H. Miller, V. Masson-Delmotte, A.E. Sveinbjörnsdottir, J. White, Oxygen isotope and palaeotemperature records

from six Greenland ice-core stations: Camp Century, Dye 3, GRIP, GISP2, Renland and NorthGRIP, Journal of Quaternary Science 16 (4) (2001) 299–307.
[40] G.C. Bond, W. Showers, M. Elliot, M. Evans, R. Lotti, I. Hajdas, G. Bonani, S. Johnson, The North Atlantic's 1–2 kyr climate rhythm: relation to Heinrich Events, Dansgaard/Oeschger Cycles and the Little Ice Age, in: P.U. Clark, R.S. Webb, L.D. Keigwin (Eds.), Mechanisms of Global Climate Change at Millennial Time Scales, Geophysical Monograph, vol. 112, AGU, Washington, DC, 1999, pp. 35–58.
[41] J. Chappell, Sea level changes forced ice breakouts in the last glacial cycle: new results from coral terraces, Quaternary Science Reviews 21 (2002) 1229–1240.
[42] M. Siddall, E.J. Rohling, A. Almogi-Labin, C. Memleben, D. Meischner, I. Schmelzer, D.A. Smeed, Sea-level fluctuations during the last glacial cycle, Nature 423 (2003) 853–858.
[43] I. Cacho, J.O. Grimalt, C. Pelejero, M. Canals, F.J. Sierro, J.A. Flores, N.J. Shackleton, Dansgaard–Oeschger and Heinrich Event imprints in Alboran Sea paleotemperatures, Paleoceanography 14 (6) (1999) 668–705.
[44] J.P. Sachs, S.J. Lehman, Subtropical North Atlantic temperatures 60,000 to 30,000 years ago, Science 286 (1999) 756–759.
[45] K.M. Cuffey, G.D. Clow, R.B. Alley, M. Stuiver, E.D. Waddington, R.W. Saltus, Large arctic temperature change at the Wisconsin–Holocene glacial transition, Science 270 (1995) 455–458.
[46] P.J. Fawcett, A.M. Agustsdottir, R.B. Alley, C.A. Shuman, The Younger Dryas termination and North Atlantic deep water formation: insight from climate model simulations and Greenland ice core data, Paleocanography 12 (1997) 23–38.
[47] G. Krinner, C. Genthon, J. Jouzel, GCM analysis of local influences on ice core δ signals, Geophysical Research Letters 24 (22) (1997) 2825–2828.
[48] G. Krinner, C. Genthon, GCM simulation of the Last Glacial Maximum surface climate of Greenland and Antarctica, Climate Dynamics 14 (1998) 741–758.
[49] J. Chappellaz, J.-M. Barnola, D. Raynaud, Y.S. Korotkevich, C. Lorius, Ice-core record of atmospheric methane over the past 160,000 years, Nature 345 (1990) 127–131.
[50] E.J. Brook, T. Sowers, J. Orchardo, Rapid variations in atmospheric methane concentration during the past 110,000 years, Science 273 (1996) 1087–1091.
[51] J. Chappellaz, T. Blunier, D. Raynaud, J.M. Barnola, J. Schwander, B. Stauffer, Synchronous changes in atmospheric CH_4 and Greenland climate between 40 and 8 kyr BP, Nature 366 (1993) 443–445.
[52] Q. Zhuang, J.M. Melillo, D.W. Kicklighter, R.G. Prinn, A.D. McGuire, P.A. Steudler, B.S. Felzer, S. Hu, Methane fluxes between terrestrial ecosystems and the atmosphere at northern high latitudes during the past century: a retrospective analysis with a process-based biogeochemistry model, Global Biogeochemical Cycles 18 (GB3010) (2004), doi:10.1029/2004GB002239.
[53] A. Dällenbach, T. Blunier, J. Flückiger, B. Stauffer, J. Chappellaz, D. Raynaud, Changes in the atmospheric CH_4 gradient between Greenland and Antarctica during the last glacial and the transition to the Holocene, Geophysical Research Letters 27 (7) (2000) 1005–1008.
[54] E.J. Brook, S. Harder, J. Severinghaus, E.J. Steig, C.M. Sucher, On the origin and timing of rapid changes in atmospheric methane during the last glacial period, Global Biogeochemical Cycles 14 (2) (2000) 559–572.
[55] E.G. Nisbet, Have sudden large releases of methane from geological reservoirs occurred since the Last Glacial Maximum, and could such releases occur again? Philosophical Transactions of the Royal Society of London. A 360 (2002) 581–607.
[56] S.J. Johnsen, W. Dansgaard, On flow model dating of stable isotope records from Greenland ice cores, in: E. Bard, W.S. Broecker (Eds.), The Last Deglaciation: Absolute and Radiocarbon Chronologies, NATO ASI series, vol. I 2, Springer Verlag, 1992, pp. 13–24.
[57] J. Schwander, J.-M. Barnola, C. Andrié, M. Leuenberger, A. Ludin, D. Raynaud, B. Stauffer, The age of the air in the firn and the ice at Summit, Greenland, Journal of Geophysical Research 98 (1993) 2831–2838.
[58] M. Hutterli, R. Röthlisberger, Atmosphere-to-snow-to-firn transport studies of HCHO at Summit, Greenland, Geophysical Research Letters 26 (1999) 1691–1694.
[59] S.C. Colbeck, Air movement in snow due to windpumping, Journal of Glaciology 35 (120) (1989) 209–213.
[60] J. Severinghaus, M. Fahnestock, M. Albert, T. Scambos, C. Shuman, Do deep convective zones exist in low-accumulation firn? Geophysical Research Abstracts 6 (2004) EGS04-00821.
[61] P. Martinerie, V.Y. Lipenkov, D. Raynaud, J. Chappellaz, N.I. Barkov, C. Lorius, Air content paleorecord in the Vostok ice core (Antarctica): a mixed record of climatic and glaciological parameters, Journal of Geophysical Research 99 (1994) 10565–10576.
[62] D. Dahl-Jensen, Reconstruction of palaeo climate from temperature measurements in bore holes on the Greenland Ice Sheet, in: K. Mosegaard (Ed.), Proceedings of the Interdisciplinary Inversion Workshop 2, Copenhagen 1993, The Niels Bohr Institute for Astronomy, Physics and Geophysics, University of Copenhagen, 1993, pp. 11–14.
[63] W. Dansgaard, S.J. Johnsen, H.B. Clausen, C.C. Langway Jr., Time scale and ice accumulation during the last 125,000 years as indicated by the Greenland 18-O curve, Geological Magazine 110 (1973) 81–82.
[64] T. Sowers, M. Bender, D. Raynaud, Y.S. Korotkevich, J. Orchardo, The $\delta^{18}O$ of atmospheric O_2 from air inclusions in the Vostok ice core: timing of CO_2 and ice volume changes during the penultimate deglaciation, Paleoceanography 6 (6) (1991) 679–696.
[65] T. Sowers, M. Bender, L. Labeyrie, D. Martinson, D. Raynaud, J. J. Pichon, Y.S. Korotkevich, A 135,000-year Vostok-Specmap common temporal framework, Paleoceanography 8 (6) (1993) 737–766.
[66] J.R. Petit, J. Jouzel, D. Raynaud, N.I. Barkov, J.-M. Barmola, I. Basile, M. Bender, J. Chapppellaz, M. Davis, G. Delaygue, M. Demotte, V.M. Kotlyakov, M. Legrand, V.Y. Lipenkov, C. Lorius, L. Pépin, C. Ritz, E. Saltzman, M. Stievenard, Climate and atmospheric history of the past 420,000 years from the Vostok ice core, Antarctica, Nature 399 (1999) 429–436.
[67] J. Jouzel, N.I. Barkov, J.M. Barnola, M. Bender, J. Chappellaz, G. Genthon, V.M. Kotlyakov, V. Lipenkov, C. Lorius, J.R. Petit, D. Raynaud, G. Raisbeck, C. Ritz, T. Sowers, M. Stievenard, F. Yiou, P. Yiou, Extending the Vostok ice-core record of palaeoclimate to the penultimate glacial period, Nature 364 (1993) 407–412.
[68] M. Bender, T. Sowers, M.-L. Dickson, J. Orchardo, P. Grootes, P. A. Mayewski, D.A. Meese, Climate correlations between Greenland and Antarctica during the past 100,000 years, Nature 372 (1994) 663–666.

[69] D.A. Meese, A.J. Gow, R.B. Alley, P.M. Grootes, M. Ram, K.C. Taylor, G.A. Zielinski, J.F. Bolzan, P.A. Mayewski, E.D. Waddington, The GISP2 depth-age scale: method and results, Journal of Geophysical Research 102 (C12) (1997) 26.411–26.423.

[70] M. Bender, T. Sowers, L. Labeyrie, The dole effect and its variations during the last 130,000 years as measured in the Vostok ice core, Global Biogeochemical Cycles 8 (3) (1994) 363–376.